X-ray imaging of vortex cores in confined magnetic structures

Peter Fischer,[1,*] Mi-Young Im,[1] Shinya Kasai,[2]
Keisuke Yamada,[3] Teruo Ono,[3] and André Thiaville[4]

[1]*Center for X-Ray Optics, Lawrence Berkeley National Laboratory, 1 Cyclotron Road, Berkeley, CA 94720, USA*

[2]*Magnetic Materials Center, National Institute for Materials Science (NIMS), 1-2-1, Sengen, Tsukuba, Ibaraki, 305-0047 Japan*

[3]*Institute for Chemical Research, Kyoto University, Gokasyo, Uji 611-0011, Japan*

[4]*Laboratoire de physique des solides, Université Paris-sud, CNRS UMR 8502, Bât. 510, 91405 Orsay Cedex, France*

(Dated: April 27, 2011)

Abstract

Cores of magnetic vortices in micron-sized NiFe disk structures, with thicknesses between 150 and 50 nm, were imaged and analysed by high resolution magnetic soft X-ray microscopy. A decrease of the vortex core radius was observed, from $\sim$ 38 to 18 nm with decreasing disk thickness. By comparing with full 3D micromagnetic simulations showing the well-known barrel structure, we obtained excellent agreement taking into account instrumental broadening and a small perpendicular anisotropy. The proven magnetic spatial resolution of better than 25 nm was sufficient to identify a negative dip close to the vortex core, originating from stray fields of the core. Magnetic vortex structures can serve as test objects for evaluating sensitivity and spatial resolution of advanced magnetic microscopy techniques.

PACS numbers: 68.37.Yz,75.78.Cd,78.20.Ls,75.70.Kw

*Electronic address: PJFischer@lbl.gov

Magnetic vortex structures occur in soft ferromagnetic films and patterned elements, such as thin disks of the $Ni_{80}Fe_{20}$ alloy, as a result of the balance between exchange and dipolar energies. They are characterized by a curling magnetization in the plane of the disk with a vortex core in the center, where the magnetization points perpendicular to that plane. Two binary properties are commonly used to describe the vortex structure: the chirality, i.e. the counter-clockwise or clockwise curling of the in-plane magnetization, and the polarity, i.e. the up or down direction of the vortex cores magnetization. The static [1–6] and dynamic [7–13] properties of these objects have recently attracted an increased scientific interest both for fundamental and applied reasons. For example, magnetic vortex structures were suggested as potential future high-density and non-volatile recording systems [14–17], since the size of the vortex core is proportional to the magnetic exchange length Λ, which can extend into the sub-10 nm regime [18], and the magnetic core represents a very stable spin configuration, in fact protected by topology. However, to further advance through experimental investigations the physical understanding of magnetic vortex structures, particularly the fast dynamics of the vortex core, advanced analytical microscopic tools with high spatial and temporal resolution are required. The first experimental images of magnetic vortex cores have been obtained by magnetic force microscopy (MFM) [1] and, shortly after, the static internal structure of the vortex has been studied at almost atomic spatial resolution by spin-polarized scanning tunneling microscopy (SP-STM) [2]. In addition, the ultrafast dynamics of the vortex structure has been investigated by time-resolved Kerr microscopy [19], revealing the rich spectrum of excitations and eigenmodes of the vortex [20, 21]. Soft X-ray microscopies which utilize circularly polarized X-rays to detect magnetic circular dichroism (XMCD), providing an element-specific magnetic contrast [22], have recently proved to be of great advantage to the study of the cores of magnetic vortices [23] and their dynamics, due to the simultaneously achievable combination of high spatial [24–26] and temporal resolution. Further, in order to assess the resolution of a magnetic microscopy technique, reliable magnetic test objects with a small, adjustable and known size are indispensable. In this letter, we quantitatively evaluate for the first time the use of a vortex core as such a test object, by systematically comparing images obtained with state-of the art X-ray optics to 3D micromagnetic simulations.

The experiments have been performed at the full field soft X-ray microscope XM-1 located at beamline 6.1.2 at the Advanced Light Source (Berkeley CA), where Fresnel zone plates provide a better than 25 nm spatial resolution. Since XMCD probes the projection of the magnetic moments onto the photon propagation direction (z-direction), in perpendicular geometry the M_z component

of the vortex core magnetization is directly imaged [23]. It shows up as dark or white contrast in the center of the disk, depending on whether the vortex core points in or out of the disk plane. Since the X-ray source at this instrument is a bending magnet, left and right polarization can be obtained by blocking the upper or lower half of the cone of the emitted X-rays. To suppress non-magnetic background contributions and enhance magnetic contrast, two images each with an illumination time of a few seconds were recorded with left and right polarization and then divided by each other.

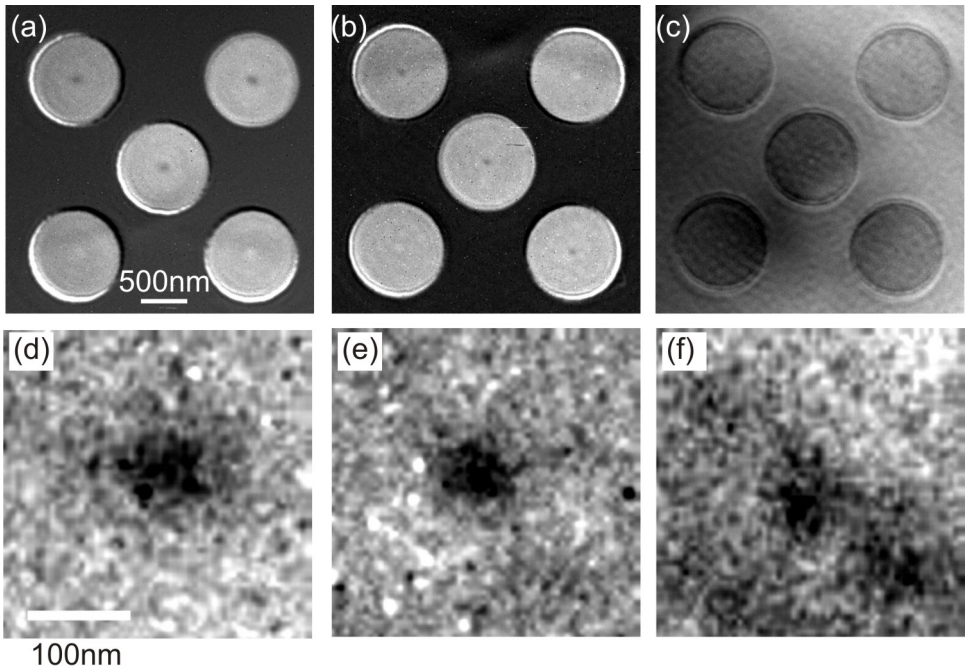

FIG. 1: Magnetic transmission soft X-ray microscopy images of permalloy disks with 500 nm radius and film thickness 150 nm (a), 100 nm (b) and 50 nm (c). The magnetic vortex cores can be identified by the black/white spots in the center, where the z-component of the magnetization of the black vortex cores points into the paper plane and out for the white cores. Detailed views of some vortex cores, one for each thickness, are shown in (d)-(f).

Samples were arrays of few permalloy ($Ni_{80}Fe_{20}$, hereafter NiFe) disks, with a constant radius of 500 nm and varying thicknesses between 150 and 50 nm. The structures were defined by e-beam lithography and subsequent e-beam evaporation of NiFe onto 100 nm thick Si_3N_4 membranes, to allow for sufficient X-ray transmission. The vortex core profiles were computed through 3D micromagnetic simulations using the public OOMMF code [27]. The mesh size was $4 \times 4 \times a$ nm^3 (with a close to 4 and adjusted with respect to the sample thickness), which is below the

micromagnetic exchange length Λ in order to describe the core structure precisely [28], and with a 3D meshing so as to describe the vortex core structure along the sample thickness. From these 3D structures, radially averaged M_z profiles were evaluated, both at the surface of the disks, at a mid-thickness plane and with thickness averaging.

The magnetic soft X-ray transmission microscopy (MTXM) images of an array of five dots with 500 nm radius and thicknesses 50, 100 and 150 nm, are shown in Fig. 1(a)-(c), respectively. While the in-plane curling magnetization does not show up in this perpendicular imaging geometry, the dark and white spots in the center of the dots, which represent the vortex cores, are clearly visible. Fig. 1(d)-(f) is a zoom into the center of some disks, i.e. the vortex core is displayed only. To analyze the M_z profile of the vortex, radially averaged intensity scans around the center of some individual dots are displayed in Fig. 2(a), (c) (white cores) and 2(b), (d) (black cores). Each radius step of 1 nm in the intensity scans is displayed by a single black dot. These profiles show a decrease of the vortex core radius W (measured by the half-width at half-maximum size, HWHM) from ~ 38 to 18 nm with decreasing disk thickness from 150 to 50 nm. Interestingly, with increasing thickness a dip develops around the vortex core and the core intensity increases. The statistics on the five-dot groups in Fig. 1 also reveal some scatter in core intensity and dip amplitude. Dot to dot variations may be ascribed to illumination non-uniformities. The observed decrease of the signal/noise ratio for smaller sample thickness is a measure of the sensitivity of the technique.

Micromagnetic calculations were performed using the commonly assumed parameters for NiFe: spontaneous magnetization $M_s = 800$ kA/m and exchange constant $A = 13$ pJ/m, so that the exchange length reads $\Lambda = \sqrt{2A/(\mu_0 M_s^2)} = 5.7$ nm here. Whereas at zero thickness the analytical profile [29] is recovered, with $W = 1.13\Lambda$, as the thickness increases the profiles adopt the "barrel" shape described by Hubert [18], with a quasi-linearly increasing width at sample mid-plane and a slightly reduced width at the surfaces. The HWHM values for the vortex core sizes W derived from that model are plotted in Fig. 3. Since only one characteristic length (exchange length Λ) is involved in this problem, Fig. 3 also shows the reduced values for the thickness h/Λ and W/Λ. As the transmitted signal in TXM averages the magnetization along the sample thickness, which is complementary to surface sensitive techniques such as scanning tunneling microscopy (STM), we use in the further discussion the HWHM of the thickness averaged intensity profiles.

These calculated profiles are superposed to the experimental data in Fig. 2 by the solid lines. In a first series of calculations (Fig. 2 (a),(b)), the NiFe was assumed to be perfectly soft, with

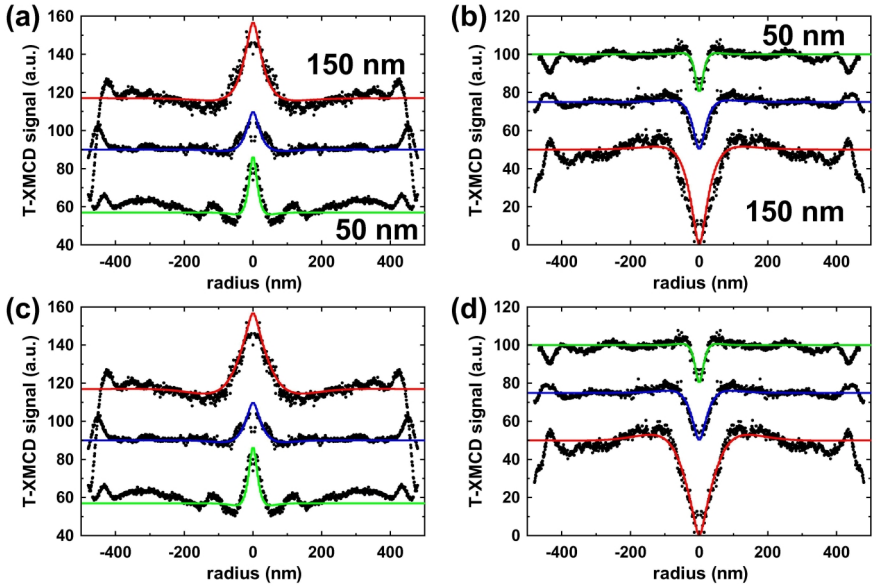

FIG. 2: Radially averaged intensity profiles for individual white (a), (c) and black (b), (d) cores (radius step 0.2 pixel $\approx$ 1 nm), for the three sample thicknesses. The solid lines (red: 150 nm, blue: 100 nm, green: 50 nm, colors online only) show the computed profiles for the thickness-averaged perpendicular magnetization, with a perpendicular anisotropy constant $K = 0$ kJ/m^3 (a), (b) and $K = 10$ kJ/m^3 (c),(d), and no instrumental broadening.

no perpendicular anisotropy. Here, the dip of opposite sign around the vortex core is extremely weak, independent of the thickness. The physical origin of this ring of opposite perpendicular magnetization quantifies the response of the sample to the stray field from the core moment. In addition, it is found that the calculated core profile is narrower than in the experiments. In a second step, we included perpendicular anisotropy of $K = 10$ kJ/m^3 (corresponding to a moderate anisotropy field $\mu_0 H_K = 250$ G) [30] and we observed that the dip in the calculation becomes more pronounced with increasing sample thickness. The existence of a perpendicular anisotropy in NiFe films has been proposed in order to interpret the appearance of so-called weak stripes at large thickness [31]. It is due to a non-zero magnetostriction combined with residual growth-induced film stress. Adding this perpendicular anisotropy also leads to calculated core profiles that are in much better agreement with the X-ray experiments (see Fig. 2 (c), (d)), at least for the thicker films: for the two profiles at 150 nm thickness shown in Fig. 2, the regression coefficients computed on the 200 nm central disk are 0.85 (a) and 0.86 (b) without anisotropy, and increase to

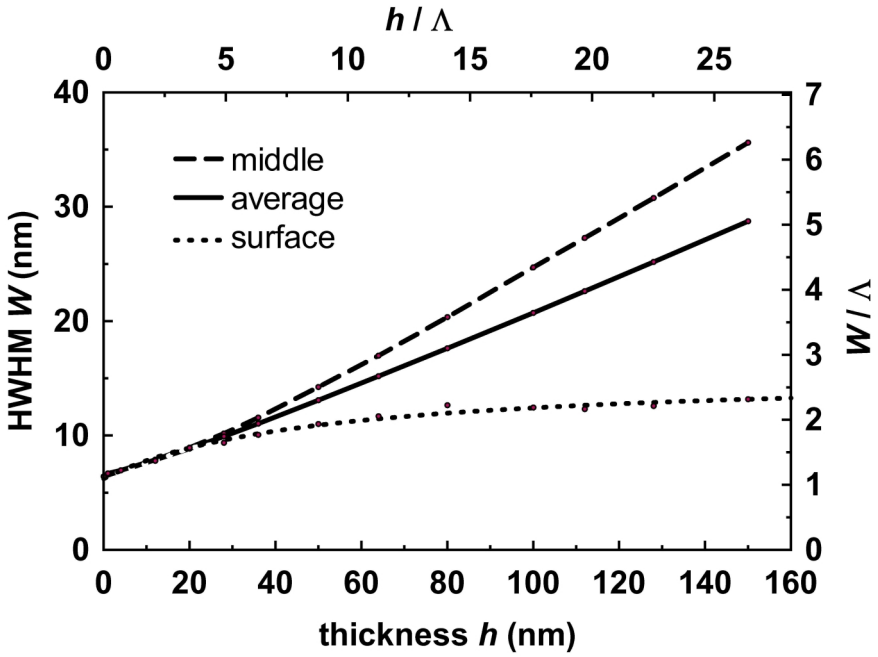

FIG. 3: HWHM values of the vortex core width W as a function of sample thickness h, evaluated by micromagnetic calculations using the radial profiles of the perpendicular magnetization component at the sample surface, mid-plane and for a thickness average. The perpendicular anisotropy is $K = 0$ kJ/m^3 and a negligible instrumental broadening is assumed ($\sigma = 1$ nm). The labels on the right and top axis give dimensions normalized to the exchange length Λ, which are the only relevant parameters for a zero anisotropy material when the disk diameter is much larger than the disk thickness.

0.93 (c) and 0.95 (d) with perpendicular anisotropy.

In order to be more systematic, a comparison of experimental and calculated core sizes is plotted in Fig. 4. The error bars in the experimental data are due to uncertainties in the thickness and to the noise level in the images. We note that the slope of core size vs. thickness is not the same for experiments and $K = 0$ calculations. In this respect, we remark that changing the micromagnetic parameters will affect in a similar proportion the two axes (in first approximation), therefore not mending this slope difference. One also observes that the perpendicular anisotropy increases the variation of core size with thickness. However, in order to account for the relatively larger core size at low thickness, it is necessary to introduce an instrumental broadening, that expresses the spatial resolution of the microscope. As can be seen in Fig. 4, a very good agreement is obtained with a Gaussian broadening having a standard deviation $\sigma = 10$ nm, corresponding

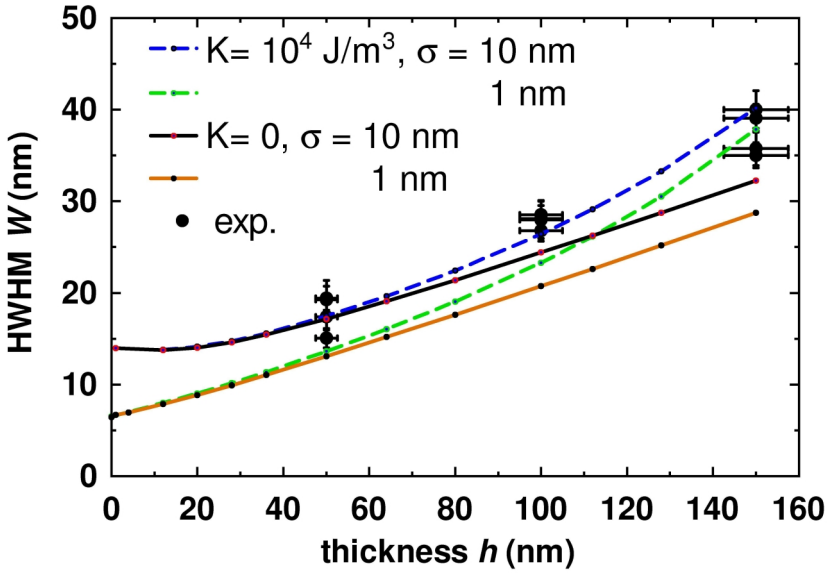

FIG. 4: Comparison of vortex core sizes as a function of sample thickness for various K-values and instrumental broadening. Dots show the experimental values with error bars (5% in thickness from preparation uncertainties, and from the 95% confidence level of the core profile fits). Lines show the micromagnetic calculations based on the thickness-averaged profiles. The cases with perpendicular anisotropy $K = 0$ kJ/m^3 (full lines) and $K = 10$ kJ/m^3 (dashed lines) are compared with, for each, a negligible instrumental broadening ($\sigma = 1$ nm) and the apparent value ($\sigma = 10$ nm).

to an instrumental gaussian FWHM of 23.2 nm, which is in full agreement with the nominal performance of the optics used in this experiment.

To conclude, we have for the first time performed a careful analysis of soft X-ray microscopy images of magnetic vortex cores in permalloy disks. Full 3D micromagnetic simulations have well reproduced the experimental data. Thus, vortex cores are suitable objects for quantifying the performance of advanced magnetic microscopy techniques. However, this requires a good knowledge of the sample parameters, including the perpendicular anisotropy. The decreasing core size with decreasing sample thickness challenges both the spatial resolution and the sensitivity of magnetic microscopy techniques, but this is the area of interest in terms of scientific and technological applications. Next generation X-ray microscopies are indeed foreseeing Fresnel zone plate optics with a spatial resolution well below 10 nm [32].

Acknowledgments

This work was supported by the Director, Office of Science, Office of Basic Energy Sciences, Materials Sciences and Engineering Division, of the U.S. Department of Energy.

---

[1] T. Shinjo, T. Okuno, R. Hassdorf, K. Shigeto, and T. Ono, Science **289**, 930 (2000).

[2] A. Wachowiak, J. Wiebe, M. Bode, O. Pietzsch, M. Morgenstern, and R. Wiesendanger, Science **298**, 577 (2002).

[3] J. Miltat and A. Thiaville, Science **298**, 555 (2002).

[4] C. Phatak, M.Tanase, A.K.Petford-Long, and M.DeGraef, Ultramicroscopy **109(3)**, 264 (2009).

[5] J. Raabe, R. Pulwey, R. Sattler, T. Schweinbock, J. Zweck, and D. Weiss, Journal of Applied Physics **88**, 4437 (2000), URL `http://link.aip.org/link/?JAP/88/4437/1`.

[6] J. K. Ha, R. Hertel, and J. Kirschner, Phys. Rev. B **67**, 224432 (2003).

[7] S. Choe, Y. Acremann, A. Scholl, A. Bauer, A. Doran, J. Stöhr, and H. A. Padmore, Science **304**, 420 (2004).

[8] J. Raabe, C. Quitmann, C. H. Back, F. Nolting, S. Johnson, and C. Buehler, Phys. Rev. Lett. **94**, 217204 (2005).

[9] K. Buchanan, P. Roy, M. Grimsditch, F. Fradin, K. Guslienko, S. Bader, and V. Novosad, Nature Phys. **1**, 172 (2005).

[10] S. Kasai, Y. Nakatani, K. Kobayashi, H. Kohno, and T. Ono, Phys. Rev. Lett. **97**, 107204 (2006).

[11] B. V. Waeyenberge, A. Puzic, H. Stoll, K. W. Chou, T. Tyliszczak, R. Hertel, M. Fähnle, H. Brückl, K. Rott, G. Reiss, et al., Nature **444**, 461 (2006).

[12] K. Yamada, S. Kasai, Y. Nakatani, K. Kobayashi, H. Kohno, A. Thiaville, and T. Ono, Nature Mater. **6**, 270 (2007).

[13] A. Vansteenkiste, K. Chou, M. Weigand, M. Curcic, V. Sackmann, H. Stoll, T. Tyliszczak, G.Woltersdorf, C. H. Back, G. Schütz, et al., Nature Physics **5**, 332 (2009).

[14] A. Drews, B. Krüger, G. Meier, S. Bohlens, L. Bocklage, T. Matsuyama, and M. Bolte, Appl. Phys. Lett. **94**, 062504 (2009).

[15] H. Jung, Y.-S. Yu, K.-S. Lee, S.-K. Kim, M.-Y. Im, P. Fischer, L. Bocklage, A. Vogel, M. Bolte, and G. Meier, Appl. Phys. Lett. **97**, 222502 (2010).

[16] M.-W. Yoo, K.-S. Lee, D.-E. Jeong, and S.-K. Kim, Phys. Rev. B **82**, 174437 (2010).

[17] Y.-S. Choi, J.-Y. Lee, M.-W. Yoo, K.-S. Lee, K. Y. Guslienko, and S.-K. Kim, Phys. Rev. B **80**, 012402 (2009).

[18] A. Hubert and R. Schäfer, *Magnetic Domains* (Springer, Berlin, 1998).

[19] J. P. Park, P. Eames, D. M. Engebretson, J. Berezovsky, and P. A. Crowell, Phys. Rev. B **67**, 020403 (2003).

[20] K. Y. Guslienko, B. A. Ivanov, V. Novosad, Y. Otani, H. Shima, and K. Fukamichi, J. Appl. Phys. **91**, 8037 (2002).

[21] K. Guslienko and V. Novosad, J. Appl. Phys. **96**, 4451 (2004).

[22] P. Fischer, D.-H. Kim, W. Chao, J. A. Liddle, E. H. Anderson, and D. T. Attwood, Materials Today **9**, 26 (2006).

[23] K. W. Chou, A. Puzic, H. Stoll, D. Dolgos, G. Schütz, B. V. Waeyenberge, A. Vansteenkiste, T. Tyliszczak, G. Woltersdorf, and C. H. Back, Appl. Phys. Lett. **90**, 202505 (2007).

[24] W. Chao, B. H. Harteneck, J. A. Liddle, E. H. Anderson, and D. T. Attwood, Nature **435**, 1210 (2005).

[25] W. Chao, J. Kim, S. Rekawa, P. Fischer, and E. Anderson, Optics Express **17(20)**, 17669 (2009).

[26] J. Vila-Comamala, K. Jefimovs, J. Raabe, T. Pilvi, R. Fink, M. Senoner, A. Maaßdorf, M. Ritala, and C. David, Ultramicroscopy **109**, 1360 (2009).

[27] M. Donahue and D. J. Porter, Tech. Rep., Interagency Report NISTIR 6376 (1999).

[28] In the zero thickness limit [29], that shows the smallest vortex core size, the magnetization angle θ with the normal axis varies with radius r as $\theta = 1.19r/\Lambda$, close to the origin. As a result, for a mesh size $a = 4$ nm and $\Lambda = 5.7$ nm, the largest angle between neighbouring cells would reach 46° (the core sitting in between mesh points). The samples measured here being thicker, the largest angle between neighbouring cells was in fact 27.5° (for the 50 nm thick sample, without perpendicular anisotropy and at the surfaces, this value falling to 5° for the 150 nm thick sample, with perpendicular anisotropy and at mid-thickness). This value is not very small, so that the vortex core energy is not precisely evaluated [33], giving rise to the well-known mesh friction effect when the core has to move. However, the cell-to-cell magnetization angle rapidly decreases away from the core center, so that the radial profile of the thickness-averaged magnetization is little affected (the considered HWHM core sizes are larger than $4a$), whereas some noise is visible in the calculated surface core widths in Fig. 3. Thus, for the smaller thicknesses calculated in Fig. 3, thinner meshes, down to $1 \times 1 \times 1$ nm^3, were used.

[29] E. Feldtkeller and H. Thomas, Phys. Kondens. Materie **4**, 8 (1965).

[30] F. Garcia, H. Westfahl, J. Schoenmaker, E. J. Carvalho, A. D. Santos, M. Pojar, A. C. Seabra, R. Belkhou, A. Bendounan, E. R. P. Novais, et al., Appl. Phys. Lett. **97** (2010).

[31] J. Ben Youssef, N. Vukadinovic, D. Billet, and M. Labrune, Phys. Rev. B **69**, 174402 (2004).

[32] W. Chao, to be published (2011).

[33] A. Thiaville, J. M. García, R. Dittrich, J. Miltat, and T. Schrefl, Phys. Rev. B **67**, 094410 (2003).

DISCLAIMER

This work was supported by the Director, Office of Science, of the U.S. Department of Energy under Contract No. DE-AC02-05CH11231.